Revisiting degron motifs in human AURKA required for its targeting by APC/C-FZR1

*Ahmed Abdelbaki[1,4,5], *Camilla Ascanelli[1], *Cynthia N. Okoye[1], Begum Akman[1,6], Giacomo Janson[2,7], Mingwei Min[1,8], Chiara Marcozzi[1,9], Anja Hagting[1,10], Rhys Grant[1,11], Maria De Luca[1], Italia Anna Asteriti[3], Giulia Guarguaglini[3], Alessandro Paiardini[2], Catherine Lindon[1]

* These authors contributed equally
1. Department of Pharmacology, University of Cambridge, Tennis Court Road, CB2 1PD, UK
2. Department of Biochemical Sciences, Sapienza University of Rome, P.le Aldo Moro 5, 00185, Rome, Italy
3. Institute of Molecular Biology and Pathology, National Research Council of Italy, c/o Sapienza University of Rome, Via degli Apuli 4, 00185 Rome, Italy
4. Current affiliation: Human Embryo and Stem Cell Laboratory, The Francis Crick Institute, 1 Midland Road, London NW1 1AT, UK
5. Current affiliation: Department of Zoology, Faculty of Science, Zagazig University, Zagazig 44519, Egypt
6. Current affiliation: Department of Biological Sciences , METU, 06800, Ankara, Turkey
7. Current affiliation: Department of Biochemistry and Molecular Biology, Michigan State University, East Lansing, Michigan 48824, United States
8. Current affiliation: Guangzhou Laboratory, Guangzhou, Guangdong 510530, China
9. Current affiliation: Centro Andaluz de Biología Molecular y Medicina Regenerativa CABIMER, Universidad de Sevilla-CSIC-Universidad Pablo de Olavide, Seville, Spain
10. Current affiliation: University of Cambridge Department of Medicine, MRC-Laboratory of Molecular Biology, Cambridge, UK
11. Current affiliation: Department of Biochemistry, University of Cambridge, Tennis Court Road, CB2 1QW, UK

Running title: Redefining AURKA degrons

Keywords: Aurora kinase, mitotic degradation, ubiquitin-mediated proteolysis, destruction box

Summary blurb: AURKA degron motifs are redefined to show that the so-called N-terminal 'A-box' is in fact a D-box, and the so-called 'D-box' in the C-terminus is not a degron but a motif critical for the active, degradable conformation of AURKA

Abstract

Mitotic kinase Aurora A (AURKA) diverges from other kinases in its multiple active conformations that may explain its interphase roles and association with cancer, and the limited efficacy of drugs targeting the kinase pocket. Regulation of AURKA activity by the cell is critically dependent on destruction mediated by the Anaphase-Promoting Complex (APC/C^{FZR1}) during mitotic exit and G1 phase and requires an atypical N-terminal degron in AURKA called the 'A-box' in addition to a reported canonical D-box degron in the C-terminus. Here we find that the proposed C-terminal D-box of AURKA does not act as a degron and instead mediates essential structural features of the protein. In living cells, as

previously reported *in vitro*, the N-terminal intrinsically disordered region (IDR) of AURKA containing the A-box is sufficient to confer FZR1-dependent mitotic degradation. Both *in silico* and *in cellulo* assays predict the QRVL Short Linear Interacting Motif (SLiM) of the A-box to be a phospho-regulated D-box. We propose that degradation of full-length AURKA additionally depends on an intact C-terminal domain because of critical conformational parameters permissive for both activity and mitotic degradation of AURKA.

Introduction

The control of mitotic exit is a paradigm for cellular regulation through targeted proteolysis. The process is orchestrated by a multi-subunit ubiquitin ligase (E3) complex, the Anaphase-Promoting Complex (APC/C), which utilizes two WD40 domain co-activator paralogues contributing to substrate recognition, CDC20 and Cdh1/FZR1 (henceforth referred to as FZR1). E3s recognise their targets through substrate motifs called degrons, and although some degrons conform to a robust consensus (for example the di-phospho-degrons recognized by SCFβTRCP), most are rather ill-defined and can usefully be defined as Short Linear Interacting Motifs (SLiMs) present in intriniscally disordered regions of proteins, or IDRs. SLiMs are proposed to adopt transient structures to mediate weak protein-protein interactions such as those between substrate and E3 ligase (Van Roey et al. 2014). Such structures have now been solved by cryoEM to identify docking sites on the APC/C for degrons known as the D-box (Destruction-Box), KEN motif and ABBA motif (Chao et al. 2012; He et al. 2013; Chang et al. 2015; Brown et al. 2016). The first D-box was identified in the N-terminal IDR of cyclin B1 (Glotzer, Murray, and Kirschner 1991), subsequently a large number have been found in other APC/C substrates, most fitting the general consensus RxxLxxxxx, although a number of variants have been identified that lack either R at position 1 (P1) or L at P4 (He et al. 2013; Davey and Morgan 2016). The KEN motif is extremely common in the proteome, first identified in CDC20 (Pfleger and Kirschner 2000) when it was thought to be specific to substrates targeted by the FZR1-activated version of the APC/C but now revealed to be a universal APC/C degron that docks onto the upper surface of the WD40 propellor of either CDC20 or FZR1 (Chao et al. 2012; He et al. 2013). The ABBA motif has been identified in BubR1 and cyclin A and confers increased affinity that is essential for control of the mitotic checkpoint (Di Fiore et al. 2015; Qin et al. 2016).

It seems likely that a combination of degrons for multivalent docking at the KEN receptor and D-box receptor (DBR) in the APC/C are required to generate selectivity in substrate targeting amongst the large number of degrons motifs present in the proteome, and to generate the increased affinity of APC/C-substrate interaction required for efficient ubiquination (Lu, Wang, and Kirschner 2015). As discussed in (Davey and Morgan 2016), lack of strict conservation of degron sequences can be explained by multivalency of degron-E3 interactions and participation of residues outside the consensus. These features go hand in hand with flexibility of IDRs, and flexibility in sequences

surrounding the degron are essential for substrate lysines to be able to mount nucleophilic attack on a nearby ubiquitin thioester linkage. The lack of sequence conservation between degrons has contributed to historic confusion in the field, with some atypical degrons described as 'novel' being subsequently redefined as variants on known degrons (i.e. they dock to the known receptor sites on the APC/C) (He et al. 2013; Davey and Morgan 2016). Indeed a systematic study of sixteen APC/C^{FZR1} substrates in budding yeast concluded that all of them depended on the DBR of FZR1 for their degradation, even when they did not have an obvious D-box (Qin et al. 2016). One candidate atypical D-box that has not been further investigated is the so-called 'A-box' of AURKA (Littlepage and Ruderman 2002).

AURKA is a substrate of the APC/C during anaphase that, unlike other anaphase substrates, is specific to the FZR1-bound form of APC/C (Honda et al. 2000; Castro, Arlot-Bonnemains, et al. 2002; Kitajima et al. 2007; Floyd, Pines, and Lindon 2008; Min et al. 2015). Potential degrons in AURKA have been defined mostly through *in vitro* studies, with deletion or mutation of either the 'A-box' motif or the putative D-box shown to stabilize AURKA against mitotic degradation in one or more assays *in vitro* or in living cells (summarized in Table 1). There is widespread acceptance in the literature that destruction of full-length AURKA depends upon an N-terminal A-box and C-terminal D-box.

However it is also well known from the crystal structure of the AURKA kinase domain that the putative D-box is located in a highly structured domain - inconsistent with the definition of a SLiM – and that its conserved RxxL residues are structurally buried (Bayliss et al. 2003). The proposed degron would therefore be inaccessible to APC/C binding unless ubiquitination of AURKA were preceded by an unfolding step, rendering problematic the designation of this motif as a degron, despite the *in vitro* evidence of degron function.

Here we describe a study undertaken to provide a more complete characterization of AURKA degrons. We report that the proposed C-terminal D-box does not display properties of a degron and instead mediates structural features of the protein essential for its normal function. We show that in living cells, as has previously been reported *in vitro* (Littlepage and Ruderman 2002), the N-terminal IDR of AURKA is sufficient to confer FZR1-dependent mitotic degradation, and that both *in silico* docking experiments and live cell degradation assays predict the so-called A-box to be an N-terminal D-box. Nonetheless degradation of full-length AURKA additionally depends on an intact C-terminal domain, because of critical conformational parameters. We propose an explanation of how mitotic degradation of AURKA is sensitive to the conformational dynamics of the substrate.

Results & Discussion

A number of publications identify putative degrons in AURKA through studies on both Xenopus and human proteins (Table 1). Since the existence of a D-box within the structured kinase domain of AURKA has been called into question (Davey and Morgan 2016; Lindon, Grant, and Min 2015), we

decided to look more closely at the putative D-box status of this motif through a combined analysis of structure, function and degradation of different AURKA mutants.

The structure of hsAURKA kinase domain (122-403) was examined in PyMol and variations in free energy resulting from different point mutations in the putative D-box (R_{371}xxL) or in an adjacent D-box-like motif (R_{375}xxL) were calculated using FoldX3 software (Figure 1). The molecular structure of the putative D-box shows L374 fitted into the hydrophobic aliphatic pocket on the kinase domain and a salt bridge established between R371 and conserved residue E299 (Figure 1A). Gibbs free energy variations (ΔΔG) for the protein folding state predict that the RxxL>AxxA substitution frequently used to test for D-box function is strongly destabilizing to the structure (R371A/L374A, ΔΔG = 5.8 kcal mol^{-1}). R371A contributes most of the free energy variation (4.9 kcal mol^{-1}) with L374A less destabilizing (ΔΔG = 2.6 kcal mol^{-1}). The conserved substitution L374I is predicted to destabilize least of all (ΔΔG = 1.6 kcal mol^{-1}) (Figure 1B).

We examined the localization of YFP- or Venus-tagged versions of AURKA in living cells and found that versions with structurally destabilizing substitutions in the R_{371}xxL motif did not behave like the wild-type (WT) protein, being excluded from (R371A/L374A) or only weakly present (R371A) on the microtubules of the mitotic spindle (Figure 1C). By contrast the less destabilizing substitution (RxxI) did not affect localization in mitotic cells. The 'non-degradable' version of AURKA (ΔA-box) generated by deletion of the N-terminal A-box degron (Littlepage and Ruderman 2002; Castro, Vigneron, et al. 2002) has previously been shown to localize as the WT protein (Floyd, Pines, and Lindon 2008; Lindon, Grant, and Min 2015). Since some versions were expressed at lower levels than the WT protein, we simultaneously depleted endogenous protein to eliminate competition from unlabelled endogenous AURKA to confirm that R371A/L374A does not localize to the spindle even when in excess over the endogenous protein (Supplementary Figure S1).

The various subcellular localizations of the Aurora kinases are known to depend on their binding partners, with the best characterized partner of AURKA, TPX2, responsible for its localization to the mitotic spindle (Kufer et al. 2002). We therefore examined the interaction of different versions of AURKA-YFP with endogenous TPX2, including the known loss of interaction mutant S155R (Bibby et al. 2009) using an in situ Proximity Ligation Assay (isPLA). As expected we found that the R371A/L374A version of AURKA, which does not localize to the mitotic spindle, does not interact with TPX2 (Figure 1D, Supplementary Figure S2). Quantification of isPLA signals confirmed that the amount of TPX2 interaction measured for different R_{371}xxL mutants (Figure 1E) correlated with the degree of spindle localization observed (Figure 1D). Probing the same versions of AURKA with antibody against the phospho-T288 epitope by immunoblot confirmed that detection of auto-activated kinase is severely compromised in R371A/L374A, as predicted for the S155R version (Figure 1F). We concluded that perturbed folding of the C-terminal region of its kinase domain prevents AURKA folding and function required for interaction with TPX2.

Next, we compared our panel of putative D-box substitutions for their effect on mitotic degradation of AURKA-Venus using a fluorescence timelapse assay. The R371A/L374A version was resistant to mitotic degradation, as is the ∆A-box version lacking the previously characterized N-terminal degron sequence located between resides 32 and 66 (Figure 2A). The R371A substitution, with partial destabilizing effect on AURKA, showed partial resistance to mitotic degradation. L374I, with the lowest ΔΔG, had no effect on mitotic degradation of the protein (Figure 2B). Plotting the amount of degradation (as percentage of each version of AURKA remaining 60 minutes after anaphase) against the calculated ΔΔG of folding revealed a significant inverse correlation of the two values (Figure 2C). These results suggested that perturbed folding could be responsible for both the deficiency in interaction with TPX2 *and* deficiency in mitotic degradation of AURKA R_{371}xxL (so-called 'D-box') mutants, and did not allow us to conclude whether or not the R_{371}xxL motif was a *bona fide* degron.

Therefore we investigated further whether the different R_{371}xxL mutations showed a pattern of mitotic degradation consistent with the designation of this motif as a D-box. Our observations that Ala substitutions at P1 and P4 of the putative D-box stabilized AURKA against mitotic degradation were consistent with the known literature on D-box motifs. However, our finding that L>I at P4 (L374I) had no effect on mitotic degradation was not consistent. An isoleucine sidechain at P4 position of a D-box would be predicted to disrupt binding to the DBR due to the shifted methyl in isoleucine that reduces the Van der Waals contribution of this residue to the interaction in the hydrophobic pocket, and should be sufficient to stabilize a substrate against APC/C-mediated degradation. Indeed, this had previously been reported for mutation of the equivalent P4 residue in Xenopus Aurora A (L381I) in *in vitro* degradation assays (see Table 1). We tested the prediction on a well-known anaphase substrate of APC/C, Polo-like kinase 1 (Plk1), whose degradation is critically dependent on a single D-box (R_{337}xxL, Figure 2D) (Lindon and Pines 2004). We introduced the single L>I substitution at P4 of the Plk1 D-box and found that this version, L340I, was unable to mediate any mitotic degradation of correctly localized Plk1 (Figure 2E). Taken together, our findings support the prediction that L>I substitution at P4 abrogates D-box function and that – since in our experiments AURKA L374I is degraded normally – the R_{371}xxL motif in human AURKA is unlikely to function as a D-box degron.

Since the C-terminal RxxL motif of AURKA was probably not a D-box, we investigated whether the N-terminal IDR would be sufficient – as well as necessary - for mitotic degradation in live cell assays. The A-box (32-66) has been shown in a number of studies to be essential for AURKA degradation in a manner that depends critically on the strongly conserved Q_{45}RVL SLiM and on the phosphorylation status of S51 (Table 1). The N-terminal K_5EN motif contributes to degradation, although since K5 is a ubiquitination site during mitotic exit (Min, Mayor, and Lindon 2013), it is not clear whether this motif acts as a degron, provides the ubiquitin receptor in the substrate, or both. We first tested AURKA(1-133) fused to GFP in live cell assays (Supplementary Figure S3) and subsequently AURKA(1-67) fused to mNeonGreen (mNeon), after confirming that the mNeon-tagged version was degraded more efficiently than the GFP-tagged version (as reported in Khmelinskii et al. 2016). We found that

AURKA(1-67) was sufficient to direct anaphase-specific, FZR1-dependent degradation of fluorescent protein tags (Figure 3A). The full-length protein was degraded more efficiently than the N-terminus alone, but we could conclude nonetheless that 1-67 of AURKA contains degrons required for its targeted destruction at mitotic exit. We further tested, in the context of AURKA(1-67), features contributing to specificity of AURKA targeting at mitotic exit, finding that both K_5EN and Q_{45}RVL SLiMs were required for degradation (Min, Mayor, and Lindon 2013)(Figure 3B). Therefore AURKA (1-67) recapitulates the known regulation of degradation of the full-length protein.

We turned to an *in silico* docking approach to examine whether the atypical Q_{45}RVL degron might bind one of the known degron receptor sites on FZR1. We docked the peptide Q_{45}RVLCPSNS into the sites on FZR1 (D-box, KEN, ABBA) identified from the cryo-EM structure of FZR1 WD40 domain bound to the pseudosubstrate domain of Acm1 (PDB:4BH6, He et al. 2013)(Figure 3C, Supplementary Figure S4), using the FlexPepDock server (Raveh, London, and Schueler-Furman 2010). The optimized pose at each site was compared with binding of a cognate degron and the Statistically Optimized Atomic Potential (SOAP) assigned to each interaction. This revealed that the Q_{45}RVL peptide favoured interaction at the D-box pocket compared to other sites, and that docking of Q_{45}RVL at this site was energetically comparable to docking of D-box peptides (Figure 3C). Comparison of the A-box with a panel of D-boxes showed that it docks with an affinity within the range of known D-boxes, although with reduced affinity compared to more canonical D-boxes (Supplementary Figure S4). We note that *in silico* docking to FZR1 alone ignores any contacts made between substrate and APC10 that probably contribute to the affinity of substrate for the D-box binding pocket (Qin et al. 2019) and therefore we may have underestimated the likely preference of Q_{45}RVL for the DBR.

The Q_{45}RVLCPSNS peptide can be docked in a similar pose to canonical D-box peptides, such that the peptide adopts a 90º turn at P4 with the leucine sidechain extending into the hydrophobic cleft in FZR1 identified by He et al. 2013 (Figure 3D), and consistent with L at P4 being the most critical residue of the D-box (He et al. 2013; Davey and Morgan 2016). We tested the importance of the leucine sidechain by making the L>I substitution at this position, the 'D-box test' predicted to disrupt docking at the DBR (and shown to block degradation of Plk1 in Figure 2D). The L48I version of AURKA(1-67) was resistant to anaphase degradation, consistent with the hypothesis that the so-called A-box (Q_{45}RVL) is a D-box (Figure 3E).

Given the conservation of R at P1 in most D-boxes, how does the AURKA Q_{45}RVL dock efficiently at the DBR? *In silico* docking predicts that some of the electrostatic interactions with E465 and D180 of FZR1, usually made by R at P1 of canonical D-boxes, could be replaced by R at P2 (Figure 4A). In He et al. (2013) it is argued that contacts made by P7 of the D-box could compensate for lack of R at P1. In AURKA, P7 of the Q_{45}xxL D-box is occupied by S51, which contacts D180 in the docking pose shown in Figure 4A. We note that in alternative poses, where the P7 residue does not contact D180 we observe steric clashes between D-box residues at P8 and P9, and APC10. A block on degradation

caused by phosphomimetic substitution at S51 has been a consistently observed feature of AURKA mitotic degradation over two decades (Table 1, Figure 4B). We confirmed in cell-based assays that S51D abrogates ubiquitination of full-length AURKA-Venus as efficiently as mutation of Q_{45}RVL or deletion of the entire A-box (32-66), pointing to a critical role of the residue in P7 in docking at the DBR (Figure 4C). We then compared *in silico* docking of wild-type A-box peptide (S at P7) with its 'non-degradable' version (D at P7) version, computing free energy values using FoldX3. This analysis confirmed increased binding energy of the mutant (Figure 4D), resulting from electrostatic repulsion between the negative charge at P7 and D180 of FZR1 (Figure 4A). The ~2.0 kcal/mol difference that we observed translates into a predicted ~30 fold increase in K_d and is consistent with the inhibition of mitotic exit degradation by S51D substitution. Our *in silico* docking model therefore explains known features of AURKA degradation and assigns the 'A-box' degron to the category of phospho-regulated D-boxes alongside securin, CDC6, KIFC1 (Holt 2012; Singh et al. 2014). We note that a recent study from the Barford lab comparing cryo-EM structures of D-boxes in Cyclin A reveals that canonical D-box D1 (RxxL) binds in a different mode to a newly identified non-canonical D-box D2 (VxxL) and that, in *in vitro* ubiquitination assays, D2 behaves as a stronger D-box degron than D1 (PDB:6Q6H, S. Zhang, Tischer, and Barford 2019). Overall, our findings are consistent with the idea that specific degron properties can be encoded in non-canonical D-boxes and that Q_{45}RVL is a APC/C^{FZR1}-specific D-box.

If all sequences required for APC/C^{FZR1}-mediated degradation of AURKA reside in its N-terminal IDR, then why does mutation in the C-terminus stabilize the full-length protein? In this study we have shown (Figure1) that the R_{371}xxL motif is required for interaction of AURKA with TPX2. Is TPX2-mediated activation of AURKA therefore required for it to be a target of APC/C? We tested this question by examining mitotic degradation of AURKA S155R-Venus (which interacts only weakly with TPX2, Figure 1E). We found that S155R was degraded with identical kinetics to the wild-type protein (Figure 5A) and concluded that interaction with TPX2 *per se* is not required for AURKA-Venus degradation. Rather, we propose that interaction of AURKA with TPX2 and with APC/C-FZR1 both depend upon a conformational state blocked by disruption of the R_{371}xxL motif in the C-terminal helix of the kinase domain.

Taken together, our results indicate that mutation in R_{371} prevents the active, degradable conformation of AURKA. An auto-inhibitory state involving interaction between the kinase domain and the N-terminus of AURKA has previously been described (Y. Zhang et al. 2007; Bai et al. 2014) and studies with a FRET-based conformational sensor confirm that the relative configuration of N- and C-terminus is altered upon activation of the kinase (Bertolin et al. 2016). Since interaction with APC/C-FZR1 occurs through an N-terminal degron motif, we propose that the Q_{45}xxL D-box is 'buried' in the inactive conformation, which may be the previously described auto-inhibited state mediated through interaction between N- and C-terminal domains (Figure 5B). Intriguingly, a heterotetrameric structure for AURKA-TPX2 captured by the Kern lab (Zorba et al. 2014) shows AURKA as a dimer stabilized by a 'dimer

swap' interaction of R371 residue with E299 in a second AURKA molecule. That is, the usual stabilizing interaction between R371 and E299 can occur in intermolecular fashion instead of intramolecular and the authors propose dimerization as a necessary step in auto-activation of the kinase (promoting autophosphorylation, allowing release of the autoinhibited state and interaction with TPX2). The most recent published studies of AURKA have described redox regulation of AURKA activity through oxidation or inhibitory CoA-lation of a cysteine residue in the kinase activation loop (Byrne et al. 2020; Tsuchiya et al. 2020) also implicated in AURKA dimerization in vitro (Zorba et al. 2014; Tsuchiya et al. 2020), indicating that there is still much to learn of the conformational complexities of AURKA.

Our own findings are consistent with the idea that R371 facilitates an activation step of AURKA and reconciles a large amount of disparate and sometimes contradictory literature on the role of the C-terminal R_{371}xxL (historically referred to as the 'D-box') in the activity, function and degradation of AURKA. In summary, we present evidence that the previously assigned 'D-box' (R_{371}xxL) of AURKA is not a degron, and that the previously named 'A-box' degron (Q_{45}RVL) is the *bona fide* AURKA D-box. Given the timing and dependencies of AURKA degradation, we propose that the A-box should be considered an APC/C-FZR1-specific D-box.

Materials and Methods

In silico mutagenesis and docking

Variation in free energy of folding upon point mutations was estimated using the FoldX programme (Guerois, Nielsen, and Serrano 2002). Docking was performed using FlexPepDock to return a docked model for each peptide tested. Where indicated, these were scored for comparison using the Statistically Optimized Atomic Potential for protein-protein docking (SOAP-PP) assigned to each interaction (Dong et al. 2013). Docking simulations at the DBR were filtered for L4 in same position as for Acm1 bound to S. cerevisiae Cdh1 (PDB code 4BH6). No positional restraints were applied when docking at the KEN/ABBA sites.

Plasmids

pVenus-AURKA-N1 has been described in previous publications (Min, Mayor, and Lindon 2013). N-terminal fragments 1-133 and 1-67 of AURKA were cloned into pEGFP-N1, with EGFP substituted by mNeon-HA for later experiments. Point mutagenesis on AURKA was carried out using standard techniques, all cloning details are available upon request.

Cell culture, synchronization and transfection

U2OS cells were cultured in DMEM supplemented with 10% FBS, 200 µM Glutamax-1, 100 U/ml penicillin, 100 µg/ml streptomycin, and 250 ng/ml fungizone (all from ThermoFisher Scientific) at 37ºC in humidified atmosphere containing 5% CO_2. Cells were transfected using a Neon electroporator

(ThermoFisher Scientific) and seeded onto 8-well microscope slides (Ibidi) for live cell imaging or onto coverslips for PLA assays.

For synchronization in mitosis, cells were treated for 12 h with 10 μM STLC (Tocris Bioscience) to trigger the Spindle Assembly Checkpoint (SAC). For mitotic exit synchronizations cells synchronized with STLC were collected by shake-off and released by 70 minute treatment with 10 μM ZM447439 (Generon, UK), an inhibitor of AURKB which ablates SAC arrest.

Fluorescence Microscopy of living cells

A few hours before live cell imaging of Ibidi slides, the culture medium was changed to L15 supplemented with 10% FBS, antibiotics and antimycotics. Images were acquired using an automated epifluorescence imaging platform composed of Olympus IX83 motorized inverted microscope, Spectra-X multi-channel LED widefield illuminator (Lumencor, Beaverton, OR, USA), Optospin filter wheel (Cairn Research, Faversham, UK), CoolSnap MYO CCD camera (Photometrics, Tuscon, AZ, USA), automated XY stage (ASI, Eugene, OR, USA) and climate chamber (Digital Pixel, Brighton, UK) and controlled using Micro-Manager (Edelstein et al. 2014). For mitotic degradation assays, multiple fields containing Venus-, EGFP- or mNeon-positive prophase and metaphase cells were selected. Images were then acquired every 2 mins for 2 hours using appropriate filter sets. Fluorescence levels were measured using ImageJ and degradation curves plotted in GraphPad Prism (San Diego, CA, USA), *in silico* synchronized to anaphase onset for each construct tested.

In situ Proximity Ligation Assay (isPLA)

U2OS cells were transfected with AURKA-Venus wild-type or mutant and seeded on coverslips. After 24 hours cells were fixed with 4% PFA and processed for isPLA using Duolink® In Situ Detection Orange (Sigma-Aldrich) according to manufacturer's instructions, using primary antibodies against GFP (Mouse mAb clone, #11814460001, Roche) and TPX2 (rabbit polyclonal antibody, Novus Biological). Epifluorescent images were acquired on the widefield imaging platform described above, as stacks of 500 nm step with 2×2 bin, using appropriate filter sets and 40X NA 1.3 oil objective, and exported as maximal intensity projections in ImageJ (http://rsb.info.nih.gov/ij/; National Institutes of Health, Bethesda, MD). Integrated intensities were measured and total isPLA signal quantified per mitotic cell and corrected for background.

Immunoblotting

Cells were lysed in in 1% Triton X-100, 150 mM NaCl, 10 mM Tris–HCl at pH 7.5 and EDTA-free protease inhibitor cocktail (Roche), and PhosSTOP™ inhibitor for phosphatase (Sigma-Aldrich). After 30 min on ice, the lysate was centrifuged at 14,000 rpm (4°C) for 10 min. For immunoblotting, an equal amount of protein (20 μg) were loaded into SDS-PAGE 4-12% pre-cast gradient gels. Proteins were transferred to Immobilon-P or Immobilon-FL membranes using the XCell IITM Blot Module according to the manufacturer's instructions. Membranes were blocked in PBS, 0.1% Tween-20, 5% BSA and

processed for immunoblotting. Primary antibodies for immunoblot were as follows: AURKA (1:1000; mouse mAb clone 4/IAK1, BD Transduction Laboratories), phospho-Aurora A (Thr288)/Aurora B (Thr232)/Aurora C [1:1000; XP® Rabbit mAb clone D13A11, Cell Signalling), β-tubulin (1:2000; rabbit polyclonal, Abcam ab6046), GAPDH (1:400; rabbit mAb #2118, Cell Signaling Technology). Secondary antibodies used were HRP-conjugated, or IRDye® 680RD- or 800CW-conjugated at 1:10000 dilution for quantitative fluorescence measurements on an Odyssey® Fc Dual-Mode Imaging System (LI-COR Biosciences).

Ubiquitination Assays

U2OS-bioUb cells transfected with different versions of AURKA-Venus were synchronized as described above and processed for detection of ubiquitin conjugates as previously described (Min 2013).

Statistical Analysis

Data analyses were performed in GraphPad Prism (San Diego, CA, USA). Results were analyzed with Student's t-test or Mann-Whitney U-test (non-parametric) as indicated in figure legends. Significant results are indicated as $p < 0.05$ (*), $p \leq 0.01$ (**) or $p \leq 0.001$(***). Values are stated as the mean ± standard deviations.

Data Availability

Acknowledgements

We thank Norman Davey, Laura Itzhaki and Rohan Eapen for discussions during the course of this work and many past researchers and students in the lab for their contributions to understanding AURKA degradation. This project was supported by Royal Society International Exchanges award (IES/R3/170195) to CL and GG whilst work in CL's lab was supported by Cancer Research UK (C3/A10239) and BBSRC (BB/R004137/1). Studentship support is acknowledged by AMA from Yousef Jameel Scholarship (Cambridge International Trust), by CNO from Gates Cambridge and Rosetrees Trust, by CA by AstraZeneca UK. AP is funded by Associazione Italiana Ricerca sul Cancro (AIRC MFAG id. 20447).

Author contributions

CL conceived and wrote the manuscript draft based on ideas developed in discussion with AP and GG. Experiments for the study were contributed by AMA, HBA, CA, CNO, AH, MM, CM, RG, MDL. GJ

supervised *in silico* experiments, LA supervised isPLA experiments. CL, AP, GG, GJ, CA, CO reviewed and edited the manuscript.

Conflicts of Interest

The authors declare no conflicts of interest.

References

Bai, Meirong, Jun Ni, Sunqin Shen, Jiaxue Wu, Qiang Huang, Yichen Le, and Long Yu. 2014. 'Two Newly Identified Sites in the N-Terminal Regulatory Domain of Aurora-A Are Essential for Auto-Inhibition'. *Biotechnology Letters* 36 (8): 1595–1604. https://doi.org/10.1007/s10529-014-1516-3.

Bayliss, Richard, Teresa Sardon, Isabelle Vernos, and Elena Conti. 2003. 'Structural Basis of Aurora-A Activation by TPX2 at the Mitotic Spindle'. *Molecular Cell* 12 (4): 851–62. https://doi.org/10.1016/S1097-2765(03)00392-7.

Bertolin, Giulia, Florian Sizaire, Gaëtan Herbomel, David Reboutier, Claude Prigent, and Marc Tramier. 2016. 'A FRET Biosensor Reveals Spatiotemporal Activation and Functions of Aurora Kinase A in Living Cells'. *Nature Communications* 7 (1): 12674. https://doi.org/10.1038/ncomms12674.

Bibby, Rachel Ann, Chan Tang, Amir Faisal, Konstantinos Drosopoulos, Steven Lubbe, Richard Houlston, Richard Bayliss, and Spiros Linardopoulos. 2009. 'A Cancer-Associated Aurora A Mutant Is Mislocalized and Misregulated Due to Loss of Interaction with TPX2'. *Journal of Biological Chemistry* 284 (48): 33177–84. https://doi.org/10.1074/jbc.M109.032722.

Brown, Nicholas G., Ryan VanderLinden, Edmond R. Watson, Florian Weissmann, Alban Ordureau, Kuen-Phon Wu, Wei Zhang, et al. 2016. 'Dual RING E3 Architectures Regulate Multiubiquitination and Ubiquitin Chain Elongation by APC/C'. *Cell* 165 (6): 1440–53. https://doi.org/10.1016/j.cell.2016.05.037.

Byrne, Dominic P., Safal Shrestha, Martin Galler, Min Cao, Leonard A. Daly, Amy E. Campbell, Claire E. Eyers, Elizabeth A. Veal, Natarajan Kannan, and Patrick A. Eyers. 2020. 'Aurora A Regulation by Reversible Cysteine Oxidation Reveals Evolutionarily Conserved Redox Control of Ser/Thr Protein Kinase Activity'. *Science Signaling* 13 (639): eaax2713. https://doi.org/10.1126/scisignal.aax2713.

Castro, Anna, Yannick Arlot-Bonnemains, Suzanne Vigneron, Jean-Claude Labbé, Claude Prigent, and Thierry Lorca. 2002. 'APC/Fizzy-Related Targets Aurora-A Kinase for Proteolysis'. *EMBO Reports* 3 (5): 457–62. https://doi.org/10.1093/embo-reports/kvf095.

Castro, Anna, Suzanne Vigneron, Cyril Bernis, Jean-Claude Labbé, Claude Prigent, and Thierry Lorca. 2002. 'The D-Box-activating Domain (DAD) Is a New Proteolysis Signal That Stimulates the Silent D-Box Sequence of Aurora-A'. *EMBO Reports* 3 (12): 1209–14. https://doi.org/10.1093/embo-reports/kvf241.

Chang, Leifu, Ziguo Zhang, Jing Yang, Stephen H. McLaughlin, and David Barford. 2015. 'Atomic Structure of the APC/C and Its Mechanism of Protein Ubiquitination'. *Nature* 522 (7557): 450–54. https://doi.org/10.1038/nature14471.

Chao, William C. H., Kiran Kulkarni, Ziguo Zhang, Eric H. Kong, and David Barford. 2012. 'Structure of the Mitotic Checkpoint Complex'. *Nature* 484 (7393): 208–13. https://doi.org/10.1038/nature10896.

Daub, Henrik, Jesper V. Olsen, Michaela Bairlein, Florian Gnad, Felix S. Oppermann, Roman Körner, Zoltán Greff, György Kéri, Olaf Stemmann, and Matthias Mann. 2008. 'Kinase-Selective Enrichment Enables Quantitative Phosphoproteomics of the Kinome across the Cell Cycle'. *Molecular Cell* 31 (3): 438–48. https://doi.org/10.1016/j.molcel.2008.07.007.

Davey, Norman E., and David O. Morgan. 2016. 'Building a Regulatory Network with Short Linear Sequence Motifs: Lessons from the Degrons of the Anaphase-Promoting Complex'. *Molecular Cell* 64 (1): 12–23. https://doi.org/10.1016/j.molcel.2016.09.006.

Di Fiore, Barbara, Norman E. Davey, Anja Hagting, Daisuke Izawa, Jörg Mansfeld, Toby J. Gibson, and Jonathon Pines. 2015. 'The ABBA Motif Binds APC/C Activators and Is Shared by APC/C Substrates and Regulators'. *Developmental Cell* 32 (3): 358–72. https://doi.org/10.1016/j.devcel.2015.01.003.

Dong, Guang Qiang, Hao Fan, Dina Schneidman-Duhovny, Ben Webb, and Andrej Sali. 2013. 'Optimized Atomic Statistical Potentials: Assessment of Protein Interfaces and Loops'. *Bioinformatics* 29 (24): 3158–66. https://doi.org/10.1093/bioinformatics/btt560.

Dulla, Kalyan, Henrik Daub, Renate Hornberger, Erich A. Nigg, and Roman Körner. 2010. 'Quantitative Site-Specific Phosphorylation Dynamics of Human Protein Kinases during Mitotic Progression'. *Molecular & Cellular Proteomics* 9 (6): 1167–81. https://doi.org/10.1074/mcp.M900335-MCP200.

Edelstein, Arthur D, Mark A Tsuchida, Nenad Amodaj, Henry Pinkard, Ronald D Vale, and Nico Stuurman. 2014. 'Advanced Methods of Microscope Control Using MManager Software'. *Journal of Biological Methods* 1 (2): 10. https://doi.org/10.14440/jbm.2014.36.

Floyd, Suzanne, Jonathon Pines, and Catherine Lindon. 2008. 'APC/C Cdh1 Targets Aurora Kinase to Control Reorganization of the Mitotic Spindle at Anaphase'. *Current Biology: CB* 18 (21): 1649–58. https://doi.org/10.1016/j.cub.2008.09.058.

Floyd, Suzanne, Nicola Whiffin, Maria P. Gavilan, Stefan Kutscheidt, Maria De Luca, Chiara Marcozzi, Mingwei Min, et al. 2013. 'Spatiotemporal Organization of Aurora-B by APC/CCdh1 after Mitosis Coordinates Cell Spreading through FHOD1'. *Journal of Cell Science* 126 (Pt 13): 2845–56. https://doi.org/10.1242/jcs.123232.

Glotzer, Michael, Andrew W. Murray, and Marc W. Kirschner. 1991. 'Cyclin Is Degraded by the Ubiquitin Pathway'. *Nature* 349 (6305): 132–38. https://doi.org/10.1038/349132a0.

Guerois, Raphael, Jens Erik Nielsen, and Luis Serrano. 2002. 'Predicting Changes in the Stability of Proteins and Protein Complexes: A Study of More Than 1000 Mutations'. *Journal of Molecular Biology* 320 (2): 369–87. https://doi.org/10.1016/S0022-2836(02)00442-4.

He, Jun, William C.H. Chao, Ziguo Zhang, Jing Yang, Nora Cronin, and David Barford. 2013. 'Insights into Degron Recognition by APC/C Coactivators from the Structure of an Acm1-Cdh1 Complex'. *Molecular Cell* 50 (5): 649–60. https://doi.org/10.1016/j.molcel.2013.04.024.

Holt, Liam J. 2012. 'Regulatory Modules: Coupling Protein Stability to Phopshoregulation during Cell Division'. *FEBS Letters* 586 (17): 2773–77. https://doi.org/10.1016/j.febslet.2012.05.045.

Honda, Kei, Hirotsugu Mihara, Yuzo Kato, Akio Yamaguchi, Hirofumi Tanaka, Hideyo Yasuda, Koichi Furukawa, and Takeshi Urano. 2000. 'Degradation of Human Aurora2 Protein Kinase by the Anaphase-Promoting Complex-Ubiquitin-Proteasome Pathway'. *Oncogene* 19 (24): 2812–19. https://doi.org/10.1038/sj.onc.1203609.

Khmelinskii, Anton, Matthias Meurer, Chi-Ting Ho, Birgit Besenbeck, Julia Füller, Marius K. Lemberg, Bernd Bukau, Axel Mogk, and Michael Knop. 2016. 'Incomplete Proteasomal Degradation of Green Fluorescent Proteins in the Context of Tandem Fluorescent Protein Timers'. Edited by Mark J. Solomon. *Molecular Biology of the Cell* 27 (2): 360–70. https://doi.org/10.1091/mbc.e15-07-0525.

Kitajima, Shojiro, Yasusei Kudo, Ikuko Ogawa, Masaaki Tatsuka, Hidehiko Kawai, Michele Pagano, and Takashi Takata. 2007. 'Constitutive Phosphorylation of Aurora-A on Ser51 Induces Its Stabilization and Consequent Overexpression in Cancer'. Edited by Nils Cordes. *PLoS ONE* 2 (9): e944. https://doi.org/10.1371/journal.pone.0000944.

Kufer, Thomas A., Herman H.W. Silljé, Roman Körner, Oliver J. Gruss, Patrick Meraldi, and Erich A. Nigg. 2002. 'Human TPX2 Is Required for Targeting Aurora-A Kinase to the Spindle'. *Journal of Cell Biology* 158 (4): 617–23. https://doi.org/10.1083/jcb.200204155.

Lindon, Catherine, Rhys Grant, and Mingwei Min. 2015. 'Ubiquitin-Mediated Degradation of Aurora Kinases'. *Frontiers in Oncology* 5: 307. https://doi.org/10.3389/fonc.2015.00307.

Lindon, Catherine, and Jonathon Pines. 2004. 'Ordered Proteolysis in Anaphase Inactivates Plk1 to Contribute to Proper Mitotic Exit in Human Cells'. *Journal of Cell Biology* 164 (2): 233–41. https://doi.org/10.1083/jcb.200309035.

Littlepage, Laurie E., and Joan V. Ruderman. 2002. 'Identification of a New APC/C Recognition Domain, the A Box, Which Is Required for the Cdh1-Dependent Destruction of the Kinase Aurora-

A during Mitotic Exit'. *Genes & Development* 16 (17): 2274–85. https://doi.org/10.1101/gad.1007302.

Lu, Ying, Weiping Wang, and Marc W. Kirschner. 2015. 'Specificity of the Anaphase-Promoting Complex: A Single-Molecule Study'. *Science (New York, N.Y.)* 348 (6231): 1248737. https://doi.org/10.1126/science.1248737.

Min, Mingwei, Ugo Mayor, and Catherine Lindon. 2013. 'Ubiquitination Site Preferences in Anaphase Promoting Complex/Cyclosome (APC/C) Substrates'. *Open Biology* 3 (9): 130097. https://doi.org/10.1098/rsob.130097.

Min, Mingwei, Tycho E. T. Mevissen, Maria De Luca, David Komander, and Catherine Lindon. 2015. 'Efficient APC/C Substrate Degradation in Cells Undergoing Mitotic Exit Depends on K11 Ubiquitin Linkages'. *Molecular Biology of the Cell* 26 (24): 4325–32. https://doi.org/10.1091/mbc.E15-02-0102.

Nguyen, Hao G., Dharmaraj Chinnappan, Takeshi Urano, and Katya Ravid. 2005. 'Mechanism of Aurora-B Degradation and Its Dependency on Intact KEN and A-Boxes: Identification of an Aneuploidy-Promoting Property'. *Molecular and Cellular Biology* 25 (12): 4977–92. https://doi.org/10.1128/MCB.25.12.4977-4992.2005.

Pfleger, C. M., and M. W. Kirschner. 2000. 'The KEN Box: An APC Recognition Signal Distinct from the D Box Targeted by Cdh1'. *Genes & Development* 14 (6): 655–65.

Plotnikova, Olga V., Elena N. Pugacheva, Roland L. Dunbrack, and Erica A. Golemis. 2010. 'Rapid Calcium-Dependent Activation of Aurora-A Kinase'. *Nature Communications* 1 (1): 64. https://doi.org/10.1038/ncomms1061.

Qin, Liang, Dimitrius Santiago P.S.F. Guimarães, Michael Melesse, and Mark C. Hall. 2016. 'Substrate Recognition by the Cdh1 Destruction Box Receptor Is a General Requirement for APC/CCdh1-Mediated Proteolysis'. *Journal of Biological Chemistry* 291 (30): 15564–74. https://doi.org/10.1074/jbc.M116.731190.

Qin, Liang, Arda Mizrak, Dimitrius Santiago P.S.F. Guimarães, Hana M. Tambrin, David O. Morgan, and Mark C. Hall. 2019. 'The Pseudosubstrate Inhibitor Acm1 Inhibits the Anaphase-Promoting Complex/Cyclosome by Combining High-Affinity Activator Binding with Disruption of Doc1/Apc10 Function'. *Journal of Biological Chemistry* 294 (46): 17249–61. https://doi.org/10.1074/jbc.RA119.009468.

Raveh, Barak, Nir London, and Ora Schueler-Furman. 2010. 'Sub-Angstrom Modeling of Complexes between Flexible Peptides and Globular Proteins: Sub-Angstrom Modeling of Flexible Peptides'. *Proteins: Structure, Function, and Bioinformatics* 78 (9): 2029–40. https://doi.org/10.1002/prot.22716.

Singh, S. A., D. Winter, M. Kirchner, R. Chauhan, S. Ahmed, N. Ozlu, A. Tzur, J. A. Steen, and H. Steen. 2014. 'Co-Regulation Proteomics Reveals Substrates and Mechanisms of APC/C-Dependent Degradation'. *The EMBO Journal* 33 (4): 385–99. https://doi.org/10.1002/embj.201385876.

Stewart, Scott, and Guowei Fang. 2005. 'Destruction Box–Dependent Degradation of Aurora B Is Mediated by the Anaphase-Promoting Complex/Cyclosome and Cdh1'. *Cancer Research* 65 (19): 8730–35. https://doi.org/10.1158/0008-5472.CAN-05-1500.

Tsuchiya, Yugo, Dominic P. Byrne, Selena G. Burgess, Jenny Bormann, Jovana Baković, Yueyang Huang, Alexander Zhyvoloup, et al. 2020. 'Covalent Aurora A Regulation by the Metabolic Integrator Coenzyme A'. *Redox Biology* 28 (January): 101318. https://doi.org/10.1016/j.redox.2019.101318.

Van Roey, Kim, Bora Uyar, Robert J. Weatheritt, Holger Dinkel, Markus Seiler, Aidan Budd, Toby J. Gibson, and Norman E. Davey. 2014. 'Short Linear Motifs: Ubiquitous and Functionally Diverse Protein Interaction Modules Directing Cell Regulation'. *Chemical Reviews* 114 (13): 6733–78. https://doi.org/10.1021/cr400585q.

Zhang, Suyang, Thomas Tischer, and David Barford. 2019. 'Cyclin A2 Degradation during the Spindle Assembly Checkpoint Requires Multiple Binding Modes to the APC/C'. *Nature Communications* 10 (1): 3863. https://doi.org/10.1038/s41467-019-11833-2.

Zhang, Yue, Jun Ni, Qiang Huang, Weihua Ren, Long Yu, and Shouyuan Zhao. 2007. 'Identification of the Auto-Inhibitory Domains of Aurora-A Kinase'. *Biochemical and Biophysical Research Communications* 357 (2): 347–52. https://doi.org/10.1016/j.bbrc.2007.03.129.

Zorba, Adelajda, Vanessa Buosi, Steffen Kutter, Nadja Kern, Francesco Pontiggia, Young-Jin Cho, and Dorothee Kern. 2014. 'Molecular Mechanism of Aurora A Kinase Autophosphorylation and Its Allosteric Activation by TPX2'. *ELife* 3 (May): e02667. https://doi.org/10.7554/eLife.02667.

Figure Legends

Figure 1: The C-terminal R_{371}xxL motif of AURKA plays a critical role in folding and function

A-B *In silico* testing of the C-terminal D-box-like motif. **A** R_{371}xxL motif is buried within the kinase domain. Arginine residue R371 (orange) establishes salt bridges with conserved glutamic acid residue E299 (green). Leucine L374 fits into the hydrophobic aliphatic pocket on the kinase domain. **B** interactions shown in **A** are lost in structures predicted for R371A and L374A substitutions. Gibbs free energy variations ($\Delta\Delta G = \Delta G_{mut} - \Delta G_{wt}$) for the protein folding state were predicted using FoldX3 software and show that R371A and L374A substitutions are more strongly destabilizing to the structure than the conserved substitution L374I. **C-E** Characterisation of different versions of Venus-tagged AURKA in human U2OS cells. **C** Panels showing localization of AURKA-Venus in live cells during interphase and at mitosis. **D-E** Interaction with TPX2 assayed by isPLA (see also Supplementary Figure 2). **D** isPLA signal reveals AURKA-Venus-TPX2 interaction on mitotic spindles. **E** Total isPLA signal was quantified per mitotic cell and corrected for background. Data for each condition ($n \geq 10$) was plotted in a scatter plot with bar and whiskers to indicate mean and SDs. Normality was verified by D'agostino and Pearson test and each mutant compared to the wild type by Ordinary One-way Anova. **, $p \leq 0.01$; ***, $p \leq 0.001$; ****, $p \leq 0.0001$. Results representative of two identical repeats of the experiment. **F** Different versions of AURKA-Venus from transiently transfected U2OS cells arrested in mitosis were probed for pT288-AURKA by immunoblot. Blot representative of two experiments.

Figure 2: The R_{371}xxL motif is not a D-box

A-B *In cellulo* mitotic degradation assays of AURKA-Venus. Graphs show quantified Venus levels from fluorescence timelapse imaging of single cells undergoing mitotic exit. Venus levels from individual cells are normalized against the Venus level at anaphase onset and *in silico* synchronized so that mean & SDs can be plotted for each version of AURKA-Venus. **A** Mutations predicted to cause disruption of the C-terminus block AURKA degradation during mitotic exit: R371A/L374A (top graph, $n \geq 10$ cells, pooled from two experiments) blocks degradation of AURKA-Venus in a similar way to deletion of the N-terminal A-box (bottom graph, $n \geq 6$ cells, from a single experiment)(Floyd, Pines, and Lindon 2008). **B** The conservative substitution L374I has no effect on kinetics of degradation of AURKA-Venus ($n \geq 10$ cells, pooled from two experiments). **C** Correlation plot for percentage degradation of each version of AURKA-Venus versus predicted $\Delta\Delta G$ of substituted residues in R_{371}xxL. **D** Schematic of known and proposed degrons in AURKA and Plk1. **E** *In cellulo* mitotic degradation assays of YFP-Plk1 WT and L341I version ($n \geq 10$ cells, pooled from two experiments). The L>I substitution at P4 of the R_{337}xxL motif abrogates degradation at mitotic exit whilst having no effect on localization of the protein (right hand panels).

Figure 3: The Q_{45}RVL motif within the AURKA A-box displays properties of a D-box degron

A-B *In cellulo* mitotic degradation assays for full-length AURKA-mNeon and AURKA(1-67)-mNeon expressed in U2OS or FZR1^{KO} U2OS cells. mNeon levels from individual cells are normalized against the anaphase onset level and *in silico* synchronized so that mean and SDs can be plotted for each protein (n ≥ 20 cells pooled from ≥ 3 experiments). Degradation curves show that (**A**) residues 1-67 are sufficient for mitotic exit-specific FZR1-dependent degradation and (**B**) mitotic degradation of AURKA(1-67)-mNeon depends on SLiMs at K_5 and Q_{45}RVL. **C** Energetics of *in silico* docking of proposed AURKA degrons into known binding pockets on FZR1, scored by SOAP-PP, using FlexPepDock server. **D** A-box (QRVLCPSNS) peptide docked to the *H.s.* FZR1 DBR (top panel), modelled upon structure PDB 4BH6 that shows *S.c.* Cdh1 bound to D-box peptide (RIALKD). PDB 4BH6 is shown for comparison in the bottom panel (He et al. 2013). **E** *In cellulo* mitotic degradation assays of AURKA-Venus WT and L48I (L>I at P4 of A-box motif, n = 26 cells pooled from two experiments).

Figure 4: Modelling of the Q_{45}RVL motif at the DBR explains the role of AURKA S51 phosphorylation

A Docking of Q_{45}RVLPSNSS peptide on FZR1. Predicted pose for QRVL in the DBR by *in silico* docking, showing orientation of the P4 Leucine and novel contacts afforded at P2 and P7. **B** *In cellulo* mitotic degradation assays of AURKA-Venus WT and S51D. **C** Ubiquitination of wild-type and different versions of AURKA carrying mutations in the A-box, transiently expressed Venus-tagged proteins were purified from U2OS cells synchronized in mitotic exit and blotted for GFP (in green) and ubiquitin conjugates (FK1 antibody, in red). Relative ubiquitination was plotted as the ratio of ubiquitin-conjugated:unmodified protein, normalized against the wild-type protein, error bars show SDs from 3 repeats of the experiment. **D** Free energy values for WT and S51D peptides computed using FoldX3. *In silico* docking models were rebuilt using mutant peptide QRVLCPDNS, models were scored with FoldX3 and the average binding free energies of 10 models for each were plotted. The higher binding energy of the mutant is significant according to Mann-Whitney test (p = 0.0147).

Figure 5: R_{371}xxL motif plays a critical role in conformational regulation of AURKA

A *In cellulo* mitotic degradation assays of AURKA-Venus WT and S155R. Venus levels from individual cells are normalized against the anaphase onset level and *in silico* synchronized so that mean and SDs can be plotted for each protein (n ≥ 10 cells, representative of two experiments). **B** Schematic proposing that the link between R371 and degradability of AURKA are mediated by a conformational step that simultaneously activates AURKA (leading to phosphorylation on T288) and makes it degradable by APC/C. The Q_{45}RVL motif is 'buried' in the autoinhibited state of the WT protein (green) and once released is autoregulated by phosphorylation on S51. The R371A mutant (orange) is unable to undergo the critical conformational step required for both activation and degradation.

Table 1 Summary of AURKA degrons described in the scientific literature

reported AURKA degron			Evidence *in vitro*	Evidence in cells	Notes
Name	position				
	Xenopus	Human			
D-box[1]	R378		Arlot-Bonnemains 2001		RxxL>RxxI stabilizes in CSF extract assay
			Castro 2002a		RxxL>AxxA stabilizes and reduces FZR1-dependent ubiquitination
			Littlepage 2002a		1-386 or RxxL>AxxL are stable versions
		R371	Crane 2004		*in vitro* degradation assays
				Kitajima 2007	sensitivity to FZR1 overexpression
KEN[2]	K6		Arlot-Bonnemains 2001 Littlepage 2002a		very small effect on degradation, not thought to be a degron
		K5	Crane 2004		very small effect on degradation, not thought to be a degron
				Min 2014	identifed as ubiquitinated residue
A-box	34-69		Littlepage 2002a		1-136 sufficient for degradation
	44-55		Castro 2002b		A-box behaves as 'D-box Activating Domain' (DAD)
		32-65	Crane 2004		*in vitro* degradation assays
				Floyd 2008	live cell mitotic degradation
QRVL[2]		Q45	Crane 2004		*in vitro* degradation assays
				Kitajima 2007	sensitivity to FZR1 overexpression.
Phospho-site[3]	S53		Littlepage 2002a Littlepage 2002b Castro 2002b		phospho-mimic versions stable in *in vitro* degradation assays.
		S51	Crane 2004		phospho-mimic versions stable in *in vitro* degradation assays.
				Kitajima 2007 Lindon 2016	sensitivity to FZR1 overexpression. live cell mitotic degradation.

1 Also shown for AURKB D-box *in vitro* in (Stewart and Fang 2005) but not in (Nguyen et al. 2005).
2 Identified as degron in AURKB (Nguyen et al. 2005).
3 pS51 found in proteomic studies as *bone fide* phosphorylation site (Daub et al. 2008; Dulla et al. 2010; Plotnikova et al. 2010).

FIGURE 1

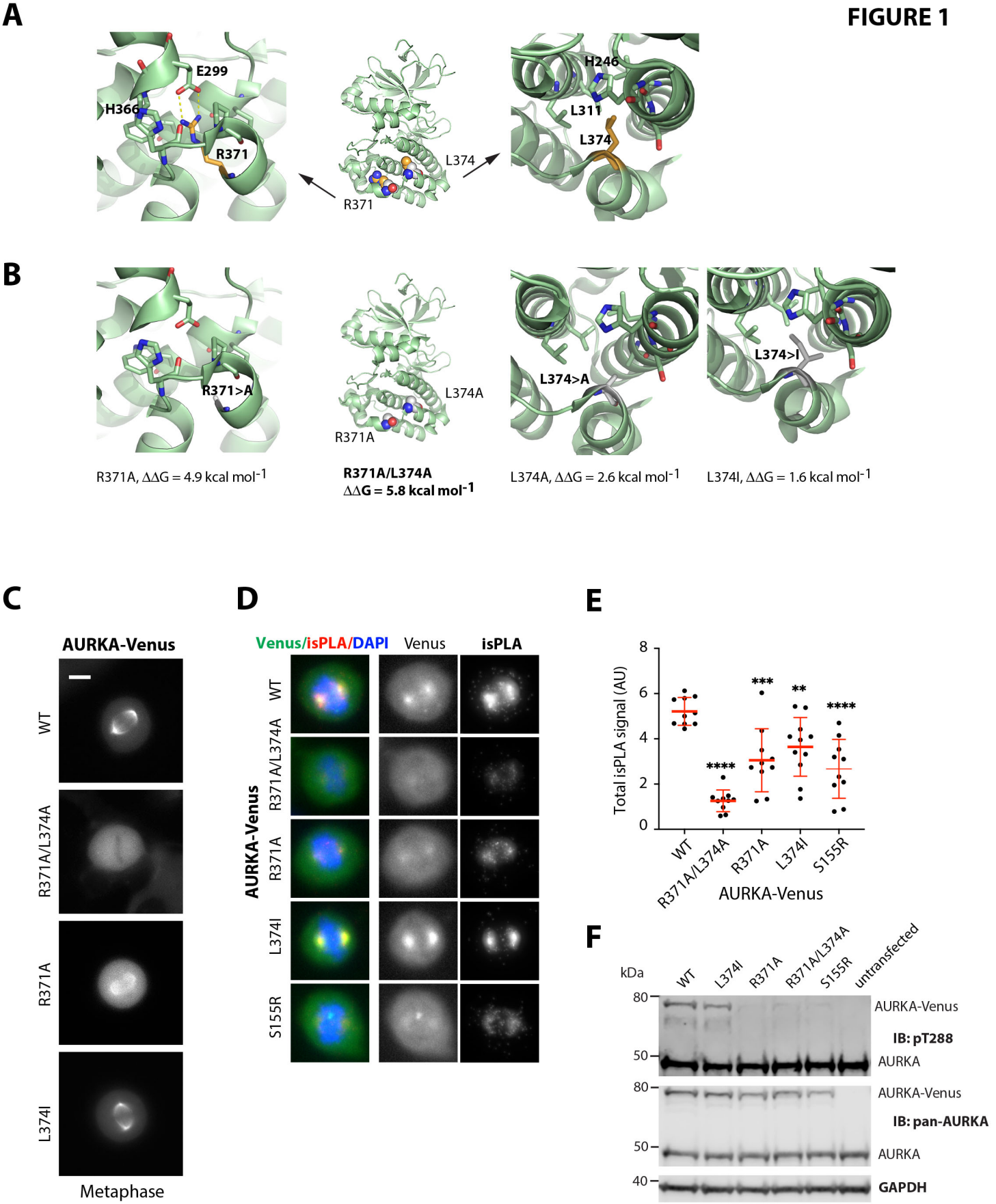
A
E299
H366
R371
R371
L374
H246
L311
L374
B
R371>A
R371A, ΔΔG = 4.9 kcal mol-1
L374A
R371A
R371A/L374A
ΔΔG = 5.8 kcal mol-1
L374>A
L374A, ΔΔG = 2.6 kcal mol-1
L374>I
L374I, ΔΔG = 1.6 kcal mol-1
C
AURKA-Venus
WT
R371A/L374A
R371A
L374I
Metaphase
D
Venus/isPLA/DAPI
Venus
isPLA
AURKA-Venus
WT
R371A/L374A
R371A
L374I
S155R
E
Total isPLA signal (AU)
8
6
4
2
0
****
***
**
****
WT
R371A/L374A
R371A
L374I
S155R
AURKA-Venus
F
kDa
WT
L374I
R371A
R371A/L374A
S155R
untransfected
80
50
AURKA-Venus
IB: pT288
AURKA
80
50
AURKA-Venus
IB: pan-AURKA
AURKA
40
GAPDH

FIGURE 2

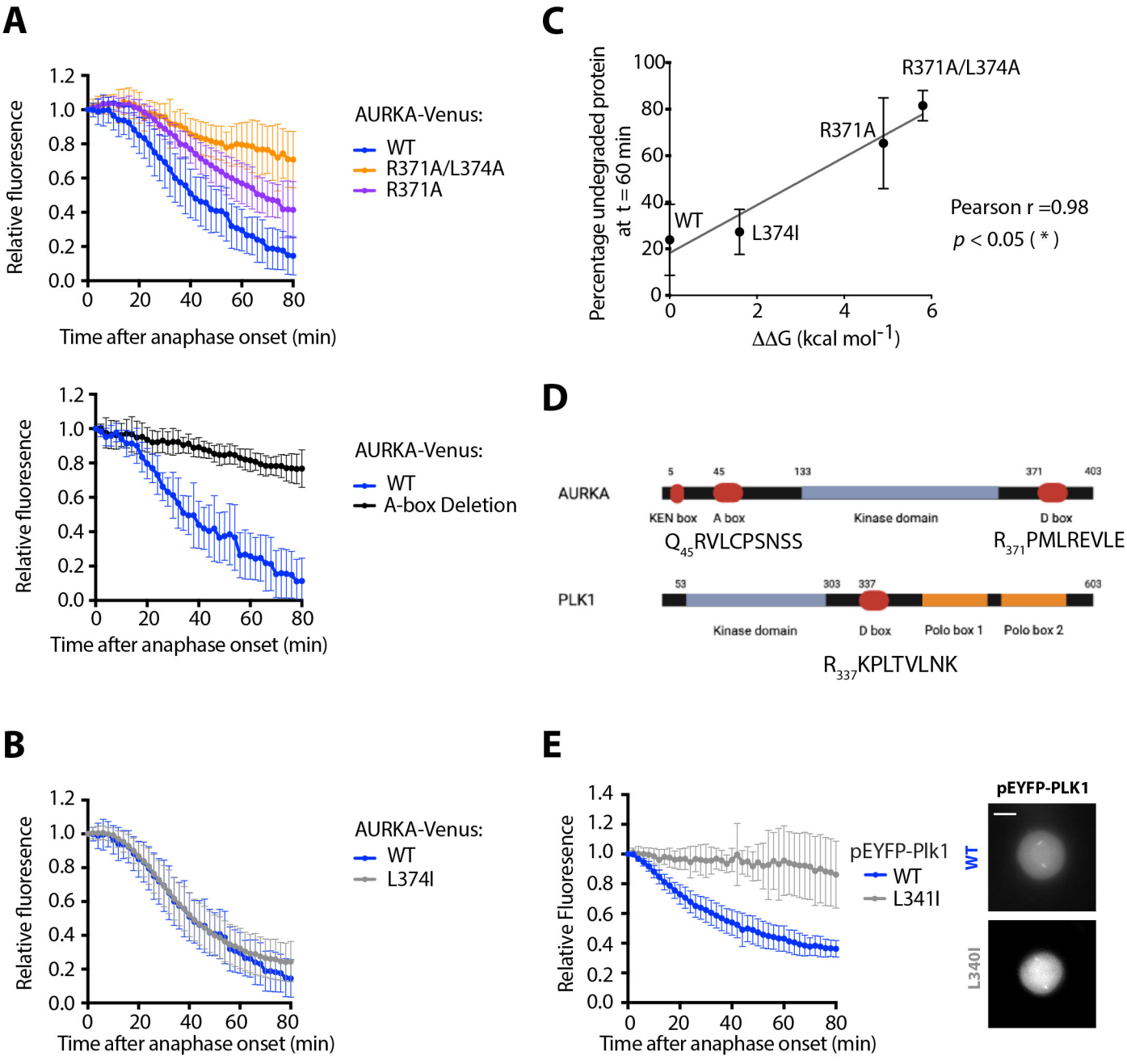
A
Relative fluoresence
Time after anaphase onset (min)
AURKA-Venus:
WT
R371A/L374A
R371A
Relative fluoresence
Time after anaphase onset (min)
AURKA-Venus:
WT
A-box Deletion
B
Relative fluoresence
Time after anaphase onset (min)
AURKA-Venus:
WT
L374I
C
Percentage undegraded protein at t = 60 min
ΔΔG (kcal mol-1)
R371A/L374A
R371A
WT
L374I
Pearson r =0.98
p < 0.05 (*)
D
AURKA
KEN box
A box
Kinase domain
D box
Q45RVLCPSNSS
R371PMLREVLE
PLK1
Kinase domain
D box
Polo box 1
Polo box 2
R337KPLTVLNK
E
Relative Fluoresence
Time after anaphase onset (min)
pEYFP-Plk1
WT
L341I
pEYFP-PLK1
WT
L340I

FIGURE 3

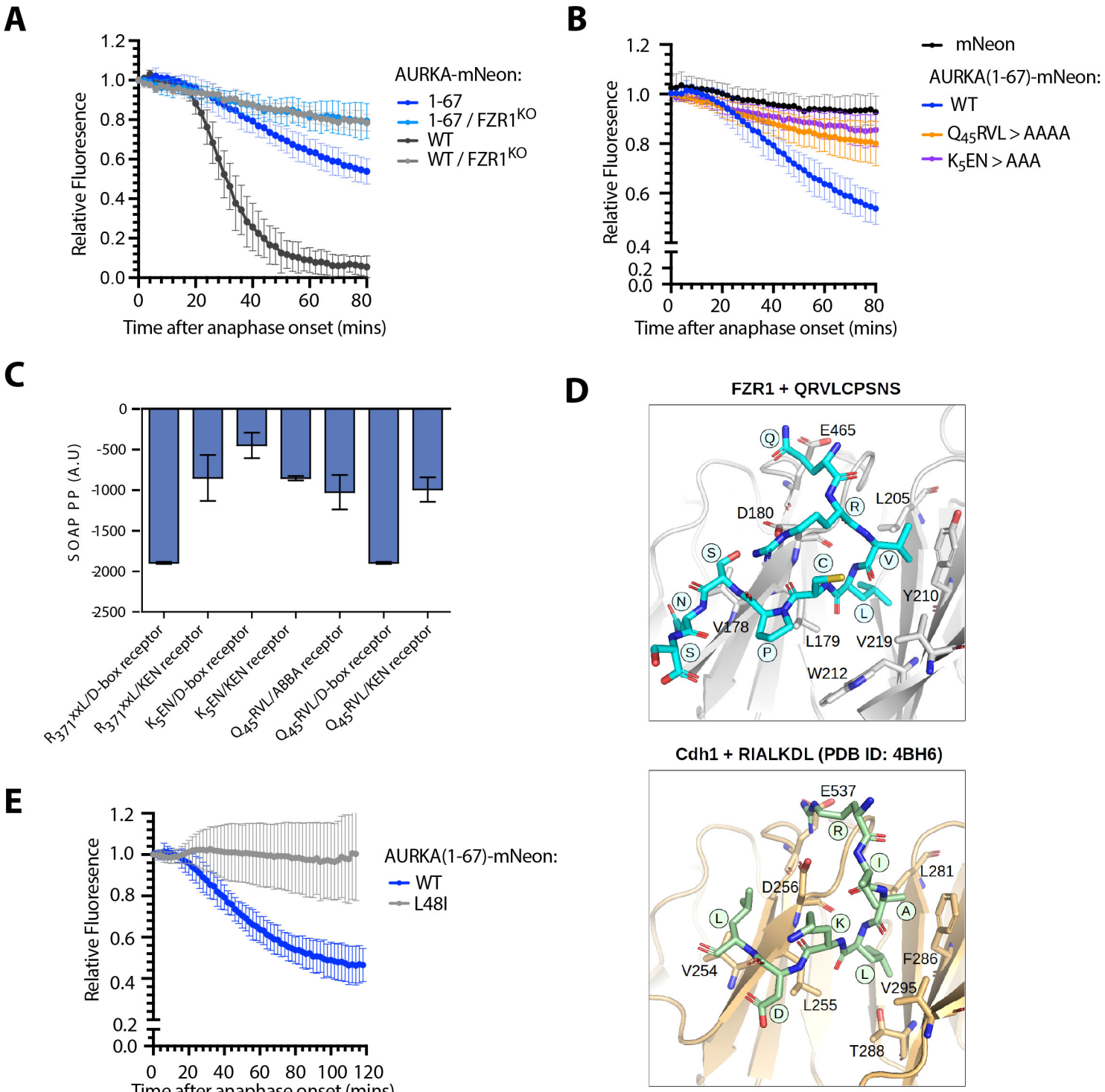
A
Relative Fluoresence
Time after anaphase onset (mins)
AURKA-mNeon:
1-67
1-67 / FZR1KO
WT
WT / FZR1KO
B
Relative Fluoresence
Time after anaphase onset (mins)
mNeon
AURKA(1-67)-mNeon:
WT
Q45RVL > AAAA
K5EN > AAA
C
SOAP PP (A.U)
R371xxL/D-box receptor
R371xxL/KEN receptor
K5EN/D-box receptor
K5EN/KEN receptor
Q45RVL/ABBA receptor
Q45RVL/D-box receptor
Q45RVL/KEN receptor
D
FZR1 + QRVLCPSNS
E465
D180
L205
Y210
V178
L179
V219
W212
Cdh1 + RIALKDL (PDB ID: 4BH6)
E537
D256
L281
V254
L255
F286
V295
T288
E
Relative Fluoresence
Time after anaphase onset (mins)
AURKA(1-67)-mNeon:
WT
L48I

FIGURE 4

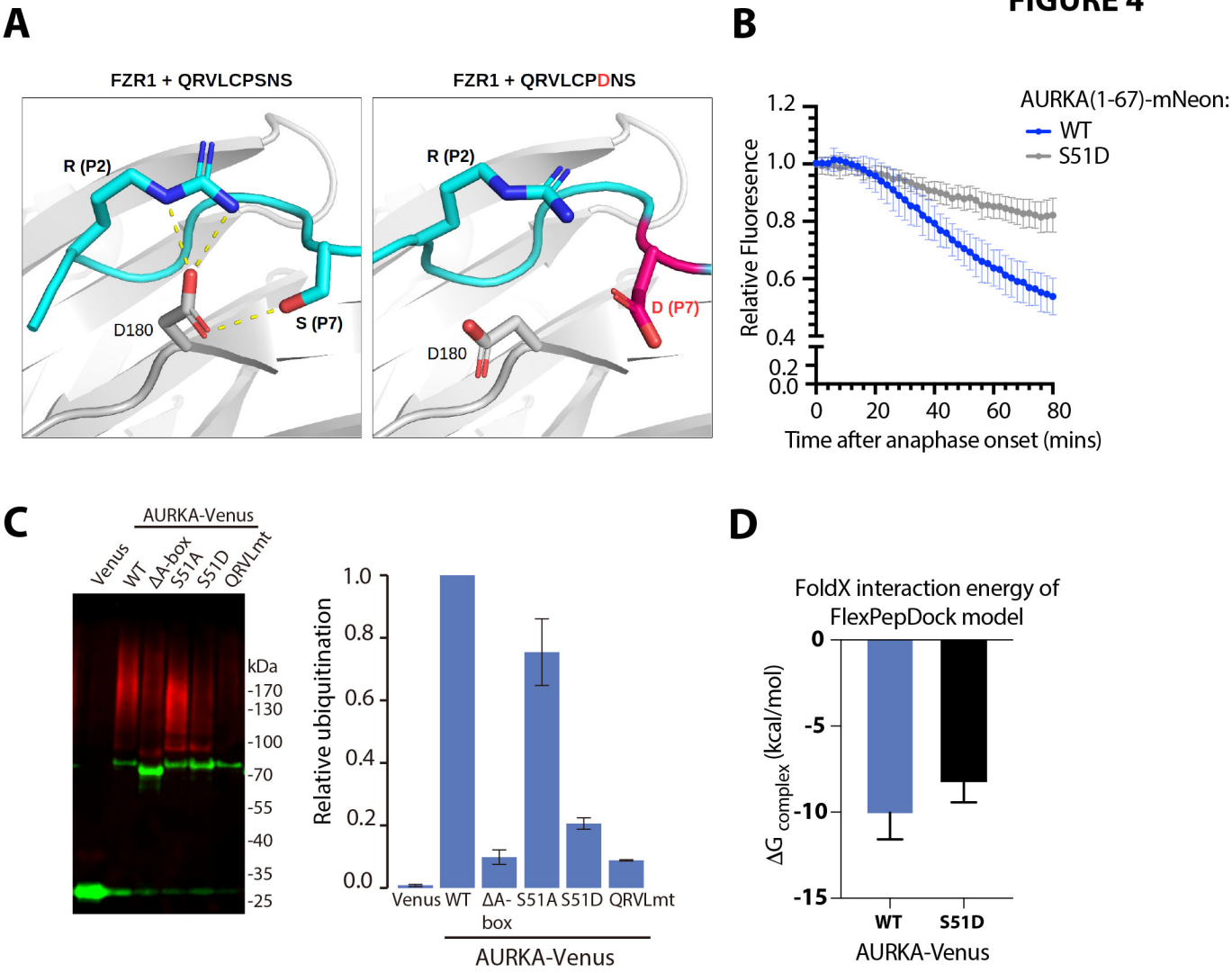
A
FZR1 + QRVLCPSNS
FZR1 + QRVLCPDNS
R (P2)
D180
S (P7)
D (P7)
B
AURKA(1-67)-mNeon:
WT
S51D
Relative Fluoresence
Time after anaphase onset (mins)
C
AURKA-Venus
Venus
WT
ΔA-box
S51A
S51D
QRVLmt
kDa
-170
-130
-100
-70
-55
-40
-35
-25
Relative ubiquitination
D
FoldX interaction energy of
FlexPepDock model
ΔG complex (kcal/mol)
WT
S51D
AURKA-Venus

FIGURE 5

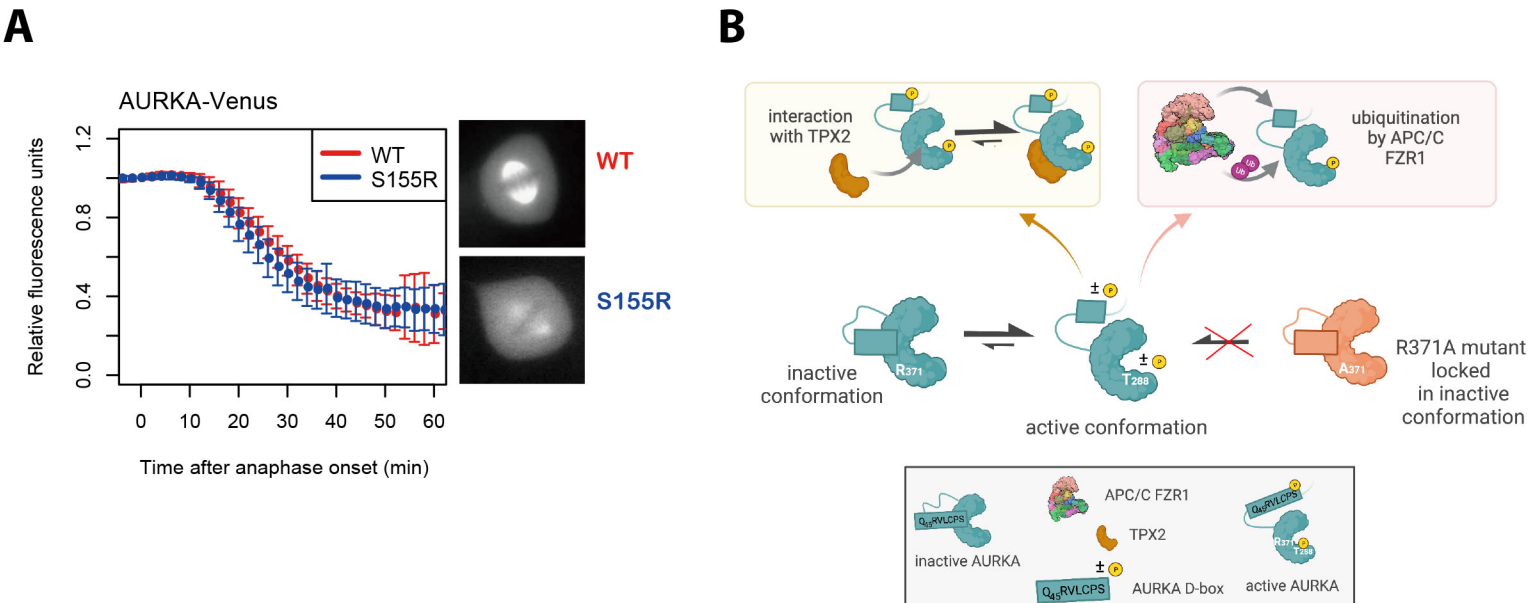
A
AURKA-Venus
Relative fluorescence units
0.0
0.4
0.8
1.2
0
10
20
30
40
50
60
Time after anaphase onset (min)
WT
S155R
WT
S155R
B
interaction with TPX2
ubiquitination by APC/C FZR1
inactive conformation
active conformation
R371A mutant locked in inactive conformation
R371
T288
A371
APC/C FZR1
TPX2
inactive AURKA
AURKA D-box
active AURKA